to appear in S.A. Benton, ed., SPIE Proc. Vol. #1914: *Practical Holography VII,* (Feb. 1992) paper 1914-27.

ADVANCES IN HOLOGRAPHIC VIDEO

Pierre St-Hilaire, Stephen A. Benton, Mark Lucente,
John D. Sutter, Wendy j. Plesniak

Spatial Imaging Group
MIT Media Laboratory
Cambridge, MA

ABSTRACT

We discuss recent developments in the MIT electronic holography display. These include the use of multiple galvanometric scanners as the horizontal scanning element, two 18-channel acousto-optic modulators (AOM's) working in tandem, and a bank of custom-designed high-bandwidth framebuffers. We also describe some recent progress on computational issues.

I ACOUSTO OPTIC MODULATORS

The basic idea underlying the MIT electronic holography display is the use of an acousto-optic modulator (AOM) as a dynamic display medium[1,2]. The holographic information is first computed at suitable sampling intervals and then converted to a high bandwidth analog signal with a modified video display framebuffer. Those samples are then frequency shifted, amplified and fed to the AOM transducer. The transducer converts the electrical signal into a phase modulation that propagates down the AOM crystal as shear waves. Laser light diffracted by the phase pattern is then scanned in a raster fashion by a combination of galvanometric X and Y scanners and the resulting hologram is imaged in front of an output lens. Because the AOM is a 1-dimensional device, the displayed holograms exhibit horizontal parallax only.

The general direction of our recent research has been towards the parallelization of the computational and display processes. We believe that large displays can be implemented with available technologies if we take a massively parallel approach.

The first logical step in that direction is to increase the number of available channels in the AOM since the space bandwidth product of the display scales linearly with the number of acoustic channels. Previous experiments with 3 channels AOM's[3] met with success and convinced us of the feasibility of an 18-channel display. The design of that element was developed in conjunction with NEOS Corp. (Melbourne, FL). The two AOM's used in our newer design use shear mode TeO_2 as the acousto-optic material. Each acoustic channel is 2 mm wide and the interchannel distance is 4 mm. The interchannel crosstalk is less than 30 dB and each channel has a space-bandwith product of 1000. The RF bandwidth of the AOM's ranges from 55 to 105 MHz.

II OPTICAL SCANNING

2.1 Problem definition

The limitations of the polygonal scanning approach described in a previous paper[1] become evident if we describe how the design parameters scale with image size and horizontal view zone. We will consider here the case where the horizontal scanning element coincides with the Fourier transform of the AOM phase pattern, i.e., the focal point of lens L_1 of Fig. 1. At the scanning plane, the size of this Fourier transform is given by:

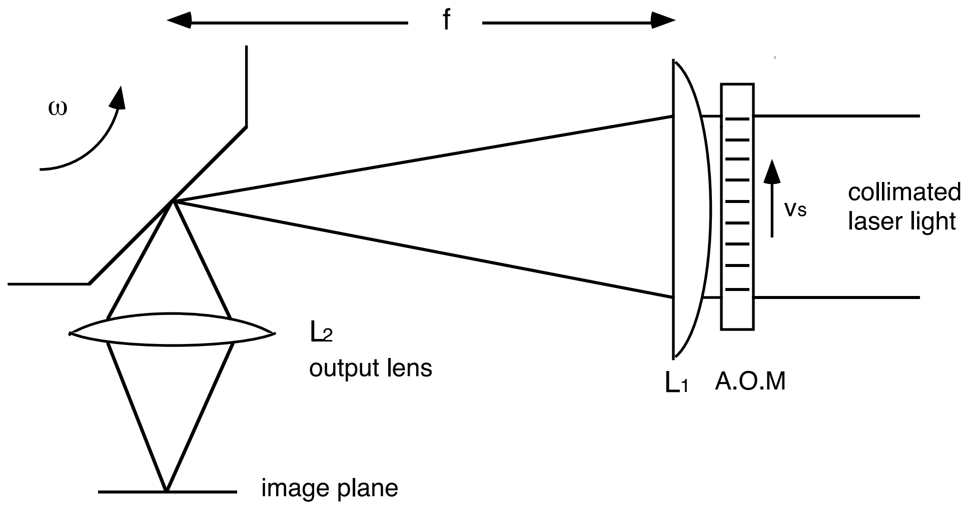

figure 1. Horizontal scan geometry

$$\Delta x = \lambda f \, \Delta f_s = \lambda f \frac{\Delta\nu}{v} , \tag{1}$$

where f is the focal length of lens L_1, Δf_s is the range of spatial frequencies on the AOM, v is the acoustic velocity of the AOM material and $\Delta\nu$ denotes the frequency range of the signal sent to the AOM's transducer.

The total number N_t of samples required for a single line of a horizontal parallax hologram having a horizontal size d and a view zone θ is[1]:

$$N_t = \frac{2 \, d \, \sin\theta}{\lambda} . \tag{2}$$

The frequency range of the signal sent to the AOM is related to Nt and the horizontal scan period τ by the formula:

$$\Delta\nu = \frac{N_t}{2\tau} = \frac{d \, \sin\theta}{\lambda \, \tau} . \tag{3}$$

It is thus clear from (1) and (3) that the size of the Fourier transform, and hence the size of the horizontal scanning element, is proportional to the product of the width and view angle of the desired hologram for a given horizontal scan rate. For a polygonal scanner a number of straightforward calculations lead to the following design parameters[4]:

- The polygon radius R must have a minimum value given by:

$$R \geq \frac{\lambda \, N^2 \, \tau \, \Delta\nu}{2\pi} , \tag{4}$$

where N is the number of polygon facets. Using (4) with (3) then leads to the result:

$$R \geq \frac{N^2 \; d \; \sin\theta}{2 \; \pi^2} \; . \qquad (5)$$

- The angular speed of the polygon obeys the formula:

$$\omega = \frac{2\pi}{N \; \tau} \; . \qquad (6)$$

A few numerical explorations easily demonstrate that using a polygon as the horizontal scanning element becomes impractical for images more than a few centimeters across. As an example, an image with a horizontal size of 20 cm and a view angle of 20 degree would require a polygon having a radius of 50 cm, assuming a 12-sided element spinning at 12 000 rpm.

2.2 Single galvanometric scanner display

A possible solution to this problem is to use a galvanometric scanner as the horizontal scanning element. Since we require a constant angular velocity scanning over the entire deflection range, the galvanometric scanner is fed with a triangle or sawtooth waveform. For an horizontal scanner the size of the scanning mirror is simply given by the extent of the Fourier transform Δx, which obeys the formula:

$$\Delta x = \frac{d \, \sin\theta}{2 \, \Omega} \; , \qquad (7)$$

where Ω denotes the mechanical excursion range of the galvanometric scanner. The f/number of the output lens scales linearly with the scan angle, so in practice Ω is generally kept below 15 degrees (equivalent to a 30 degrees optical deflection range).

The advantage of the galvanometric scanner approach is that the mirror size (and thus the size of the scanning section) is always much smaller than the diameter of a corresponding polygonal scanner. The main drawback comes from the lower scanning speed achievable with galvanometric scanners. The angular speed of galvanometric scanners rapidly decreases with mirror inertia (and thus size), but the requirement of a minimum display refresh rate constrains the scan rate to be in excess of 150 Hz[4]. We have found that 60 mm seems to be the upper limit for the horizontal extent of the scanning mirror for a 150 Hz scanning rate and an acceptable linearity. This assumes the use of a state of the art scanner and a lightweight beryllium mirror. The display characteristics that we acheived with such a mirror are described in Table I.

2.3 Galvanometric scanner arrays.

The limitations of the single galvanometric scanner approach can be overcome if instead we use an array of galvanometric scanners as our horizontal deflection system. The human visual system will not notice a decrease in image quality if the spot size of the light deflected by any single scanner is smaller than the resolving power of the eye. This can be stated in geometrical terms by requiring that the exit pupil of an image projected by each scanner be larger than the pupil of the eye and that the gap between each scanner be small compared to the eye pupil (Fig. 2). This can be stated as:

$$l_{scanner} \geq \frac{P \; f}{D_{view}} \; , \qquad (7)$$

$$l_{gap} << \frac{P\ f}{D_{view}} \quad , \tag{8}$$

where P denotes the human pupil size (typically about 3 mm), f is the focal length of the output imaging lens, and D_{view} denotes the viewing distance. Equations (7) and (8) assume a Fourier geometry but can be easily adapted to the more common Fresnel case. We note that the galvanometric scanners do not have to be phased locked for such a configuration to work.

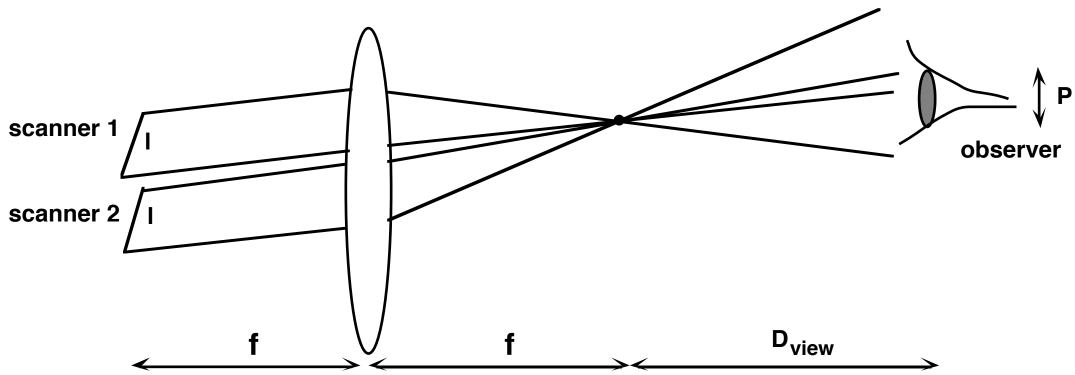

Figure 2. Multiscanner geometry

The maximum interscanner gap is a function of the mirror size and total mechanical scan excursion θ (Fig. 3). Simple trigonometric calculations yield the formula:

$$l_{gap} = l_{scan}\left(1 - \cos\left(\frac{\theta}{2}\right)\right) \tag{9}$$

In practice, however, l_{gap} will always be slightly larger than implied by (3) because of the necessary minimum clearance between mirrors.

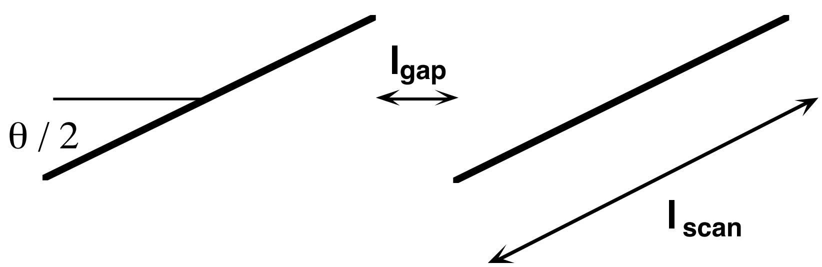

Figure 3. Interscanner gap

As an example, let us consider the tandem scanner system implemented at the Media Laboratory (Fig. 4). It consists of two scanners, each supporting a 60 mm beryllium mirror. Assuming a focal length of 160 mm for the output lens and a 500 mm view distance condition (7) requires a mirror size larger than 1 mm and is thus easily met. From (9) we get a gap of 0.5 mm assuming a 15 deg. mechanical scan angle, to which we add a 0.5 mm clearance. Condition (8) is thus barely met, and the effect of the scanner gap is noticeable upon close inspection of the image. Obviously in this case the use of a larger number of smaller mirrors would prove advantageous. The characteristics of that display are shown in Table I.

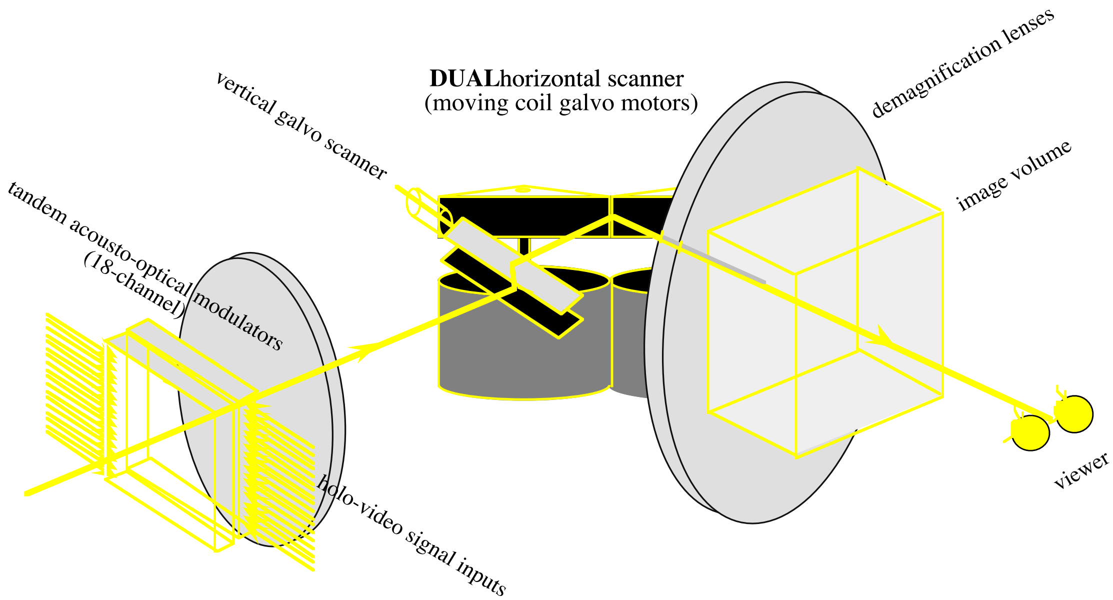

Figure 4. Tandem scanner display

III ELECTRONIC HARDWARE

A framebuffer system called "Cheops" was used to provide the 36-MB holographic pattern through 18 parallel channels. Cheops was designed at the MIT Media Laboratory to be used in the development of scalable digital television. Cheops is capable of video-rate image coding and decoding. It a modular system, composed of up to four processor boards and up to four each of the input and output modules. The Cheops system was specially modified to support the 6 output modules needed for holographic video. The output modules are basically 3-channel framebuffers, with each channel capable of holding 2 MB of data in VRAM. The output format of the framebuffers is reconfigurable. For example, for the purposes of large-scale holographic video, the data streams from the output cards were configured to be 256 KB of uninterrupted data (one holo-line) with 102 KB of blanking between each, read from the D/A converters at a 110-MHz clock rate. Because of limitations in the present optical part of the display, however, we oversampled the holographic signal by a factor of 2, resulting in an effective sample content of 128 K per horizontal line and a 25 MHz analog bandwidth.

The video signals coming from the framebuffers are frequency shifted by mixing with a local oscillator, filtered to keep only a single sideband, and amplified before being sent to the AOM's transducers. The operating range of the AOM extends from 55 to 105 MHz. A simple circuit generates the different signals used to drive the electro-mechanical part of the display. A block diagram of the system is shown in Fig. 5.

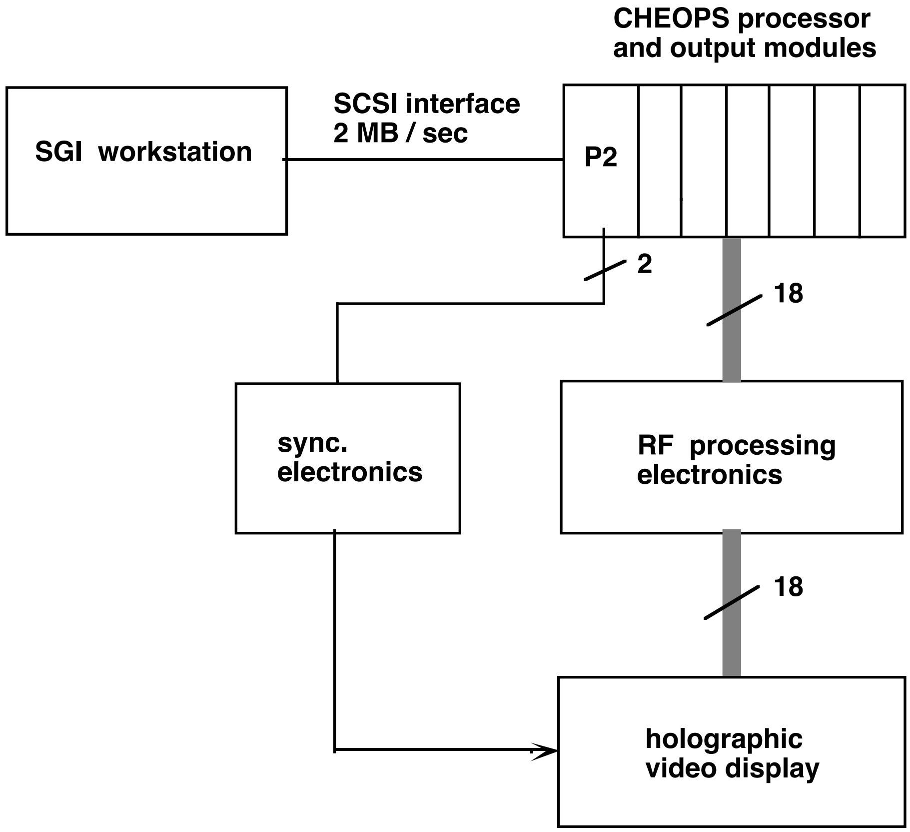

Figure 5. Block diagram of the 18-channel display

IV HOLOGRAM COMPUTATION

The simplest approach to hologram generation involved computing directly on Cheops. The computational power provided by the Cheops processor board was adequate for generating simple images. The entire 36-MB holographic fringe pattern was computed on the Cheops processor module using a lookup table approach [5,6]. This approach, described in previous articles, provides for the fastest computation of holographic fringe patterns, especially where computational power is limited. The look-up table approach begins by computing and storing in RAM memory an array of elemental holographic interference fringe patterns. Each elemental fringe represents the interference intensity contribution from an image point source at a particular depth position in the image volume. Each image point source has a brightness and an (x,y,z) location in the image volume (where x is horizontal, y is vertical, and z is depth). The processor module receives this 3D image description over the SCSI link from the SGI workstation that is used as a file server and as a link to the external network. Because the hologram possesses horizontal parallax only (HPO), an object point source contributes only to a single horizontal line (holo-line) of the CGH. During computation, a given image point is processed as follows:

- Index the look-up table using z (depth location).
- Laterally translate the indexed fringe by x (horizontal location).
- Scale the fringe amplitude by the image point brightness.
- Accumulate the resulting fringe into the holo-line indexed by y.

The linearity required to scale and add the intensity patterns was possible through the use of the bipolar intensity approach to CGH generation[5,6]. The final CGH pattern was scaled to fit into the 8-bit VRAM of the output framebuffers. As each holo-line (256KB in width) was computed, it was then sent into the appropriate portion of the framebuffer VRAM for rapid readout to the display electronics.

The i960-based Cheops processor board, though a powerful computer with (currently) 32 MB of processor RAM, was not enough to compute complex images in reasonable times. For example, an image containing only 836 points in 3D (a wireframe representation of a flowerpot) required approximately 2 minutes. Times such as these are not surprising, especially considering the absence on Cheops of any floating-point computational hardware. Specifically, the processor module lacks floating-point capabilities, trigonometric functions and square roots, all of which are essential to the computation of holographic interference patterns. In order to make computation of simple objects possible in only a few minutes, the code was designed to work around these limitations. The lookup table, computed directly on Cheops, was stored as 8-bit bytes. Computation of such a table, which represents the complex physical phenomenon of light propagation, generally requires floating-point precision and the use of trigonometric functions such as sin(x) and cos(x). Many substitutions were made to overcome this deficiency. First, trigonometric functions were generated using a polynomial expansion. For the sake of speed when computing the elemental fringe patterns, a more rapid "homemade" cosine function was used: the cosine was approximated to a precision of only 16 different phase increments per cycle, and these values were rapidly indexed from a 16-element look-up table. Computation of the CGH was performed using only 16-bit unsigned integers. To normalize the total holographic fringe pattern to fit into a single byte of the VRAM, each of its 16-bit integers were simply shifted to the right by 8 bits.

Image quality did not suffer noticeably from the limited computing power of the processor module. For example, the first cosine function table used had a precision of only 8 phase intervals per cycle. This meant that instead of smooth cosinusoidal fringes, discrete steps occurred at 8 evenly spaced intervals within each period of the elemental fringe pattern. This phase quantization produced a noticeable noise in the displayed 3D image. However, by upgrading to a 16-phase cosine, the noise was no longer visible. As an alternative to computing on the processor module, the fringe pattern was also generated on the SGI workstation, and then downloaded over the SCSI link to Cheops. Cheops transferred the 36-MB holographic pattern directly to the output VRAM. Such an approach enabled more precise computation since the SGI workstation had full floating-point mathematics, more memory and generally more computational power. Different types of holograms (volume or stereogram[5,6]) were computed using code that had already been developed for other purposes. Also, precomputed frames were compressed and stored on disk for future use. The limitation in this approach was the maximum bandwidth available in the SCSI link. The downloading of 36 MB required between 55 and 60 seconds. Though independent of image scene complexity, this time is still unacceptably long. Generation of the 36-MB fringe pattern on the SGI workstation also required a great deal of time. For example, a stereogram (view-dependent, planar image) was computed using 16 views rendered with a resolution of 160 by 144. Computation time was 5.4 minutes, with roughly 50 seconds of this time representing the writing of the final data to disk.

V RESULTS

The characteristics of the two systems described in this paper are shown in Table I along with the characteristics of a previous display which used a polygonal scanner. The resulting images exhibited a good signal to noise ratio and an excellent contrast, but suffered from minor distortions mostly due to optical aberrations of the output lens and scanner nonlinearities. Fine tuning of the two galvanometric scanners used in the tandem system so they would stay registered thorough the angular range proved to be a major challenge. The interscanner gap was barely noticeable at a normal viewing range. There is no doubt that even better results could be acheived by using a larger number of smaller mirrors for the horizontal scanning. Apart from the smaller interscanner gap, such an arrangement would operate the scanners farther away from their resonant frequency and would thus improve their dynamic characteristics

	MARK I	MARK II a	MARK II b
scanning system	polygon	single galvanometric	dual galvanometric
samples / frame (MBytes)	6	8	18
Samples / line	32 000	64 000	128 000
Number of AOM channels	3	12	18
RF bandwidth per channel (MHz)	50	15	25
Image size (mm)	50 x 35	60 x 55	60 x 70
Horizontal view angle (deg.)	14	24	38
Vertical resolution (lines)	64 (color)	96 (B & W)	144 (B & W)
Refresh rate (Hz)	38	30	30

Table I. Display characteristics for three different configurations

VI CONCLUSIONS

There is no doubt that the multiscanner/multichannel approach can be scaled up to much larger sizes by adding more acoustic channels per AOM and more mirrors in the scanning array. Since milimeter size mirrors are optimum such an array could possibly be manufactured with the silicon micromachining technologies being developed in a number of laboratories. This opens the door to large, solid state full color displays almost within reach of today's technology.

Our laboratory is now working on a next generation system which should display twice the amount of information of our tandem scanner display. Such a system comes close to commercially useful devices in term of display characteristics and should allow the start of a series of psychophysical experiments aimed at making the most of the new medium of electronic holography.

VII ACKNOWLEDGMENTS

The authors want to acknowledge the help of Mike Klug, Kevin J. Whitcomb, Brad Edelman, Rajeevan Amirtharajah., Hwesu Mpumelelo, Mike Halle, Michele Henrion, Mike Bove, and Shawn Becker, who have contributed to various parts of this project.

Research on the MIT holographic video system has been supported in part by US West Advanced Technologies Inc., the Defense Advanced Projects Research Agency (DARPA) through the Rome Air Development Center (RADC) of the Air Force System Command (under contract No. F30602-89-C-0022) and through the Naval Ordnance Station, Indian Head, Maryland (under contract No. N00174-91-C0117), and by the Television of Tomorrow research consortium of the Media Laboratory, MIT.

VIII REFERENCES

1. P. St Hilaire, S.A. Benton, M. Lucente, M. L. Jepsen, J Kollin, H. Yoshikawa, ”Electronic Display System for Computational Holography”, in SPIE Proceedings #1212 “Practical Holography IV”, (SPIE, Bellingham, WA, 1990), S.A. Benton, editor, pp 174-182.

2. P. St Hilaire, M. Lucente, S. A. Benton, "Synthetic Aperture Holography: A Novel Approach to Three Dimensional Displays", Journal of the Optical Society of America A, Vol. 9, No. 11, Nov. 1992, pp 1969 - 1977.

3. P. St-Hilaire, S.A. Benton, M. Lucente, J. Underkoffler, H. Yoshikawa, “Real-time holographic display: Improvements using a multichannel acousto-optic modulator and holographic optical elements”, SPIE Proceedings #1461 “Practical Holography V”, (SPIE, Bellingham, WA, 1991), S.A. Benton, editor, pp. 254-261.

4. M. Lucente, P. St Hilaire, S. A. Benton, D. Arias, J. A. Watlington, "New Approaches to Holographic Video", SPIE Proceedings #1732 "Holography '92", (SPIE, Bellingham, WA, 1992), paper #1732-48.

5. M. Lucente, " Optimization of hologram computation for real-time display." Practical Holography VI, Proceedings of the SPIE, 1992, Bellingham, WA, 1667-04, pages 32-43.

6. M. Lucente. Interactive computation of holograms using a look-up table. Journal of Electronic Imaging, in press.